

INTERACTION OF LASER RADIATION WITH MATTER https://doi.org/10.1070/QEL18029

The Autler–Townes effect, the Rabi frequency, and determination of characteristics of the decay of excited states in the photoionisation scheme of lutetium

A.B. D'yachkov, A.A. Gorkunov, A.V. Labozin, S.M. Mironov, V.A. Firsov, G.O. Tsvetkov, V.Ya. Panchenko

***Abstract*. The splitting of the first and second transitions in the lutetium photoionisation scheme $5d6s^2\,^2D_{3/2}-5d6s6p\,^4F^o_{5/2}-5d6s7s\,^4D_{3/2}-(53375\ cm^{-1})^o_{1/2}$ is studied in a wide range of laser radiation intensities, and the Rabi frequencies as functions of the radiation intensity are determined. Based on the results, we have obtained the decay branching coefficients of 0.54 and 0.41 for the first and second transitions, respectively.**

Keywords: *laser selective photoionisation, lutetium-177.*

1. Introduction

A detailed study of the lutetium photoionisation scheme $5d6s^2\,^2D_{3/2}-5d6s6p\,^4F^o_{5/2}-5d6s7s\,^4D_{3/2}-(53375\ cm^{-1})^o_{1/2}$ is of great practical importance, because this scheme, having high selectivity and efficiency of photoionisation of ^{177}Lu and ^{177m}Lu, can be used for the industrial production of these radionuclides in medical applications [1].

The photoionisation efficiency, as well as the choice of appropriate laser radiation intensities, depends to a large extent on the decay characteristics of the excited states. If the lifetime of the level is comparable to the duration of the laser pulse or less than it, then a significant part of the particles spontaneously leave the excited level. In this case, it is critically important whether the decay occurs back to the previous state or the particle passes into another, third-party state that does not participate in the photoionisation scheme. In the first case, the particle can be re-excited by laser radiation and further contribute to the separation product; in the second case, the particle is 'lost' and the degree of extraction of the target isotope decreases. In particular, for the scheme in question (Fig. 1), the lifetime of the first excited state $5d6s6p\,^4F^o_{5/2}$ is 472 ns [2], and the decay (for a pulse duration of 20 ns) does not significantly affect the photoionisation kinetics. Direct measurements show that the lifetime of the second excited level $5d6s7s\,^4D_{3/2}$ is 11.5 ns [3], and this makes it necessary to significantly increase the third-stage laser radiation intensity to prevent decay-related losses.

A.B. D'yachkov, A.A. Gorkunov, A.V. Labozin, S.M. Mironov, V.A. Firsov, G.O. Tsvetkov, V.Ya. Panchenko National Research Center "Kurchatov Institute", pl. Akad. Kurchatova 1, 123182 Moscow, Russia; e-mail: Tsvetkov_GO@nrcki.ru

Received 8 November 2021
Kvantovaya Elektronika **52** (4) 367–370 (2022)
Translated by I.A. Ulitkin

It is known that at high intensity, one can observe a well-registered splitting of the line – the Autler–Townes effect, and the magnitude of splitting depends on the laser radiation intensity [4]. Theoretical studies show that when a three-level atomic system is simultaneously exposed to laser radiation with frequencies ν_{12} and ν_{23} (corresponding to the first and second transitions), the populations of levels 1, 2, and 3 experience oscillations with characteristic frequencies Ω_{12} and Ω_{23}. At $\Omega_{12} \ll \Omega_{23}$, the 2–3 transition splits, and in scanning the ν_{12} frequency, two peaks in the population amplitude of the second excited state 3 are observed, divided by

$$\Delta\nu_{12} = \sqrt{(\Delta\nu_{23}^2 + \Omega_{23}^2)}, \quad (1)$$

where $\Delta\nu_{12}$ and $\Delta\nu_{23}$ are frequency detunings of laser radiation from the centres of the first and second transitions, respectively (in MHz); and Ω_{23} is the Rabi frequency of the second transition (in MHz) [5, 6]. Thus, when the laser radiation frequency is tuned to resonance with the frequency of the second transition ($\Delta\nu_{23} = 0$), the splitting turns out to be equal to the Rabi frequency, which makes it possible to experimentally measure this frequency. If state 3 may decay not only to state 2, but also to a number of other states, then measurements of the Rabi frequency at a given intensity allow one to determine the Einstein coefficient of the selected transition 3–2 and, consequently, the partial component of the decay of the excited state 3, associated exclusively with spontaneous transition to state 2, which, in combination with the integral lifetime of the level (the sum of all possible decays of state 3), gives the ratio of the decay probabilities to the previous state and to the state outside the photoionisation scheme, and makes it possible to estimate the losses associated with the decay.

2. Experiment

The splitting of ^{175}Lu transitions at the first and second stages of the $5d6s^2\,^2D_{3/2}-5d6s6p\,^4F^o_{5/2}-5d6s7s\,^4D_{3/2}-(53375\ cm^{-1})^o_{1/2}$ photoionisation scheme was studied by laser resonance ionisation mass spectroscopy (LRIMS). Resonant excitation and ionisation of atoms was performed by radiation from three pulsed single-mode dye lasers with a spectral linewidth of 100–150 MHz (FWHM) pumped by copper vapour lasers; the pulse repetition rate was 10 kHz. Photoions were detected using a commercial MS-7302 quadrupole mass spectrometer. The technical parameters and features of the experimental

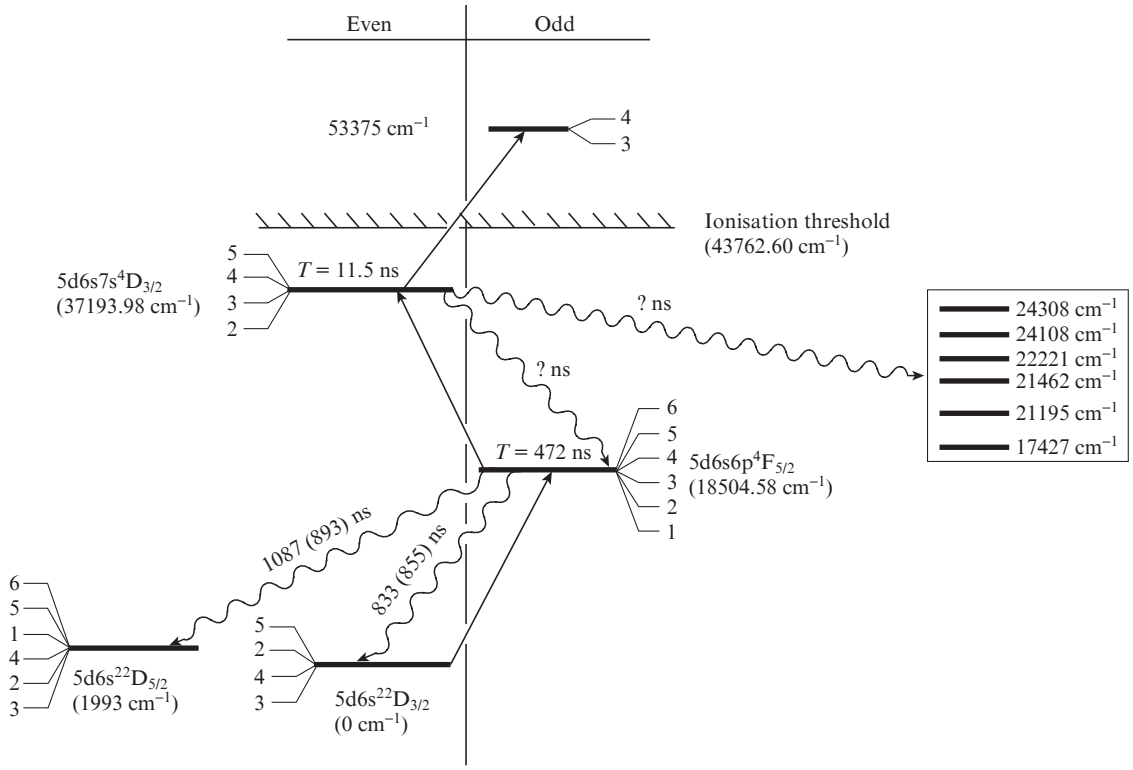

Figure 1. Scheme of photoionisation of lutetium.

setup are described in detail in [7, 8]. In the course of the study, the second-stage laser radiation frequency was tuned to resonance with the transition. The density of the average laser radiation power of the first stage decreased to 0.01 of the saturation level. The radiation wavelength of the first stage was scanned in the region of the first transition. Atoms from the second excited state were ionised into a continuum by laser radiation of the third stage with a wavelength detuned from the wavelength of the autoionisation state by 1 Å. A typical dependence of the photoion current on frequency is shown in Fig. 2, and the dependence of splitting on the average power density of laser radiation of the second stage is presented in Fig. 3.

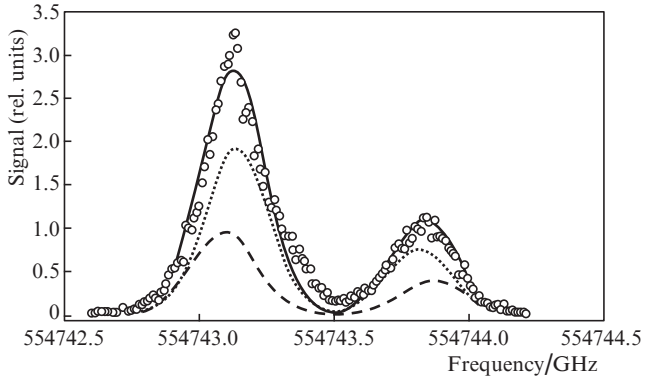

Figure 2. Splitting for the second transition 5d6s6p^{4}F$^o_{5/2}$ – 5d6s7s^{4}D$_{3/2}$ (F = 1, F' = 2). The dashed curve is the Gaussian distribution for the right and left peaks of the 00 projection, the dotted curve corresponds to projections –1–1 and 11, and the solid curve is the sum of all projections. Points show the results of the experiment.

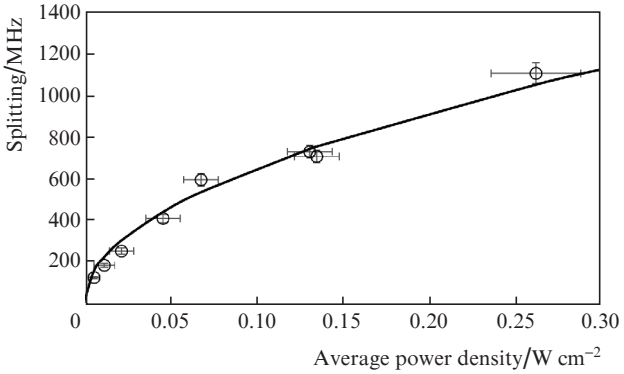

Figure 3. Dependence of the splitting for the transition 5d6s6p^{4}F$^o_{5/2}$ – 5d6s7s^{4}D$_{3/2}$ (F = 1, F' = 2) on the average power density of the second-stage laser radiation.

3. Results and discussion

To determine the relationship between the Rabi frequency of the second transition ^{4}F$^o_{5/2}$ – ^{4}D$_{3/2}$ and the decay characteristics, we used the formula for the Rabi frequency [9]

$$\hbar\Omega = |d_{FF'}E_0|, \qquad (2)$$

where $\boldsymbol{d}_{FF'}$ is the operator of the dipole moment vector of the transition from the state with the quantum number of the total mechanical moment F' to the state with the quantum number F, and $\boldsymbol{E}_0$ is the electric field of the electromagnetic wave of laser radiation. Assuming that laser radiation is a plane monochromatic wave, $E(t) = E_0\cos\omega t$, with linear

polarisation ($E_0 = \sqrt{8\pi I_L/c}$), we obtain the expression for the Rabi frequency

$$\hbar\Omega = |d_{FF'}|\sqrt{\frac{8\pi I_L}{c}}, \tag{3}$$

where $d_{FF'}$ is the projection of the dipole moment vector onto the vector $\boldsymbol{E}_0$; I_L is the intensity of laser radiation (in W cm^{-2}); and c is the speed of light (in cm s^{-1}). The matrix element of the dipole moment of the transition $d_{FF'}$ from the hyperfine structure state with quantum numbers I, J, F, and M to the state with quantum numbers I, J', F', and M' is expressed in terms of the reduced matrix element $\langle J\|D\|J'\rangle$ according to the formula [5]

$$d_{FF'} = (-1)^{F-M}\begin{pmatrix} F & 1 & F' \\ -M & 0 & M' \end{pmatrix}(-1)^{I+J+F+1}$$

$$\times\sqrt{(2F+1)(2F'+1)}\begin{Bmatrix} J & 1 & J' \\ F' & I & F \end{Bmatrix}\langle J\|D\|J'\rangle, \tag{4}$$

where M' and M are the projections of the total moments F' and F; J' and J are the quantum numbers of the total orbital and spin moments of electrons; and I is the spin of the nucleus. Elements

$$\begin{pmatrix} F & 1 & F' \\ -M & 0 & M' \end{pmatrix}, \quad \begin{Bmatrix} J & 1 & J' \\ F' & I & F \end{Bmatrix}$$

are the 3j- and 6j-Wigner symbols, respectively [10, 11]. In turn, the reduced dipole moment $\langle J\|D\|J'\rangle$ is expressed in terms of the transition characteristics [5, 12]:

$$|\langle J\|D\|J'\rangle|^2 = \frac{3\hbar\lambda^3(2J'+1)}{4\cdot 8\pi^3}A(J'\to J), \tag{5}$$

where $A(J'\to J)$ is the Einstein coefficient of the corresponding transition. The values of quantum numbers and factors in formula (4) for the studied first transition to the $5d6s6p\,^4F^o_{5/2}$ state from the $5d6s^2\,^2D_{5/2}$ metastable state and the second transition $5d6s6p\,^4F^o_{5/2} - 5d6s7s\,^4D_{3/2}$ of the ^{175}Lu atoms are presented in Table 1.

For linear polarisation ($\Delta M = 0$), transitions with three projection values are possible: $M = M' = -1, 1$ and $M = M' = 0$. Substituting the found values of the factors into (3), for the projections $M = M' = 1$ for the second transition $^4F^o_{5/2} - {}^4D_{3/2}$ ($\lambda = 5350$ Å) we obtain the frequency

$$\Omega_{23} = \Delta\nu_{12}(M = M' = 1) = \Delta\nu_{12}(M = M' = -1)$$

$$= \sqrt{\frac{1}{20}}\sqrt{\frac{3\lambda^3 P(2J'+1)}{4\pi^2\hbar cf}\frac{A_2(3/2\to 5/2)}{\tau}}, \tag{6}$$

where the laser radiation intensity

$$I_L = \frac{P}{f\tau} \tag{7}$$

is expressed in terms of the average power density P, the pulse repetition rate $f = 10$ kHz, and the effective laser pulse duration τ.

Table 1. The values of quantum numbers and factors in formula (4) for the initial and final states of the studied transitions.

Quantum numbers and factors		$^2D_{3/2} - {}^4F^o_{5/2}$ ($\lambda = 5404$ Å)	$^2D_{5/2} - {}^4F^o_{5/2}$ ($\lambda = 6055$ Å)	$^4F^o_{5/2} - {}^4D_{3/2}$ ($\lambda = 5350$ Å)
J		3/2	5/2	5/2
J'		5/2	5/2	3/2
F		2	1	1
F'		1	1	2
I		7/2	7/2	7/2
$\begin{Bmatrix} J & 1 & J' \\ F' & I & F \end{Bmatrix}$		$-\sqrt{\frac{1}{30}}$	$-\frac{1}{6}\sqrt{\frac{5}{7}}$	$-\sqrt{\frac{1}{30}}$
$\sqrt{(2F+1)(2F'+1)}$		$\sqrt{15}$	3	$\sqrt{15}$
$\begin{pmatrix} F & 1 & F' \\ -M & 0 & M' \end{pmatrix}$	11	$-\sqrt{\frac{1}{10}}$	$-\sqrt{\frac{1}{6}}$	$-\sqrt{\frac{1}{10}}$
	00	$-\sqrt{\frac{2}{15}}$	0	$-\sqrt{\frac{2}{15}}$
	–1–1	$-\sqrt{\frac{1}{10}}$	$-\sqrt{\frac{1}{6}}$	$-\sqrt{\frac{1}{10}}$

Similarly, for the projections $M = M' = 0$ we obtain

$$\Omega_{23} = \Delta\nu_{12}(M = M' = 0)$$

$$= \sqrt{\frac{1}{15}}\sqrt{\frac{3\lambda^3 P(2J'+1)}{4\pi^2\hbar cf}\frac{A_2(3/2\to 5/2)}{\tau}}. \tag{8}$$

For each scan, the experimental dependence of the signal on the frequency ν of the scanned laser radiation was approximated by the dependence

$$S(\nu) = \sum B_+ G(\nu; \nu_0 + 0.5\Omega(F, M, F', M'))$$

$$+ \sum B_- G(\nu; \nu_0 - 0.5\Omega(F, M, F', M')), \tag{9}$$

where the summation is performed over all transition projections corresponding to the condition $\Delta M = 0$ (linear polarisation); $G(\nu;\ \nu_0)$ is the Gaussian distribution with centre frequency ν_0; B_- and B_+ are amplitude multipliers (Fig. 2). Based on the results of the approximation, we obtained $A(3/2 \to 5/2)/\tau = (1.8 \pm 0.3)\times 10^{15}$ 1/s^2. For a laser pulse duration $\tau = 20$ ns, this gives the Einstein coefficient $A_2(3/2 \to 5/2) = (3.6 \pm 0.6)\times 10^7$ 1/s, which is in good agreement with the data of [13] (3.201×10^7 1/s). Thus, the partial lifetime of the second excited state $^4D_{3/2}$ with respect to the decay into the first excited state $^4F^o_{5/2}$ is 28 ± 5 ns, which corresponds to the branching coefficient of 41% ± 6% of the decay into the first excited state $^4F^o_{5/2}$.

For the first transition, approximation of the results by formula (9) gives $A_g(5/2 \to 3/2)/\tau = (1.4 \pm 0.2)\times 10^{14}$ 1/s^2 for the transition from the $^2D_{3/2}$ ground state and $A_m(5/2 \to 5/2)/\tau = (1.2 \pm 0.2)\times 10^{14}$ 1/s^2 for the transition from the $^2D_{5/2}$ metastable state (Fig. 4). Taking into account that the decay of the $^4F^o_{5/2}$ level can occur only into the ground state $^2D_{3/2}$ or into the metastable state $^2D_{5/2}$, we obtain the decay branching factor into the ground state, equal to 0.54. This value agrees well with the data of [2] (57% ± 3%) and [13] (51%). However, for

a pulse duration of 20 ns, we have the Einstein coefficients $A_g(5/2 \rightarrow 3/2) = (0.7 \pm 0.1) \times 10^6$ 1/s for the transition from the ground state and $A_m(5/2 \rightarrow 5/2) = (0.6 \pm 0.1) \times 10^6$ 1/s for the transition from the metastable state, which, in turn, gives for the first excited level $^4F^o_{5/2}$ a total lifetime $T = 770 \pm 70$ ns that contradicts the value $T = 472 \pm 24$ ns presented in [2] and the value $T = 430 \pm 20$ ns from [14]. Such a contradiction may be due to the fact that the transitions $^2D_{3/2}-{}^4F^o_{5/2}$ and $^2D_{5/2}-{}^4F^o_{5/2}$ from the ground and metastable states, respectively, are intercombination transitions, with a change in the multiplicity value from 2 to 4, and the determination of the Rabi frequency of population oscillations according to formula (3) may be incorrect. Based on the presented results, we can conclude that for the considered intercombination transitions, formula (3) gives overestimated values of the Rabi frequency.

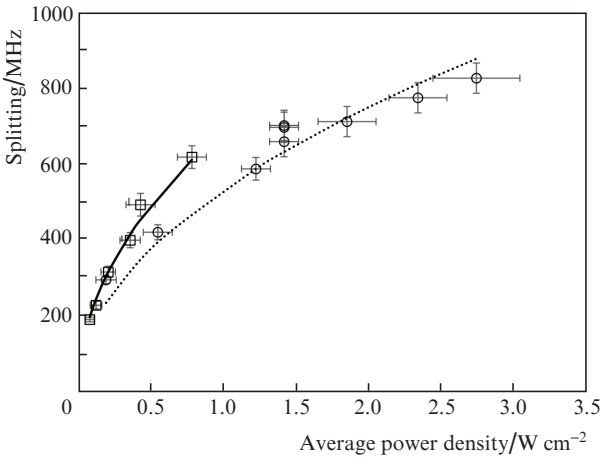

Figure 4. Dependences of the splitting on the average power density of laser radiation. The solid curve and squares correspond to the transition from the ground state $^2D_{3/2}-{}^4F^o_{5/2}(F = 1,\ F' = 2)$ with a wavelength of 5404.1632 Å, and the dashed curve and circles correspond to the transition from the metastable state $^2D_{5/2}-{}^4F^o_{5/2}(F = F' = 1)$ with a wavelength of 6056.8238 Å.

4. Conclusions

The obtained decay branching coefficients from the second excited state show that the fraction of particles that remain in the photoionisation scheme during decay is small, and the decay of the second excited state $5d6s7s^4D_{3/2}$ is the main factor limiting the degree of extraction of the target isotope due to photoionisation.

The dependences of the splitting of transitions on the laser radiation intensity, experimentally obtained in this work, characterise the measure of the coherence of the processes occurring under different regimes of lutetium photoionisation using the scheme $5d6s^2{}^2D_{3/2}-5d6s6p\,{}^4F^o_{5/2}-5d6s7s^4D_{3/2}-(53375\,\text{cm}^{-1})^o_{1/2}$. The intensities used in our work (average power density 0.01–2.5 W cm^{-2}) significantly exceed the intensities at which saturation of the photocurrent is achieved and which are used for selective photoionisation of lutetium isotopes and isomers (average power density 0.002–0.01 W cm^{-2}). As a result, it becomes clear that in the case of selective photoionisation, the Rabi frequency (and, accordingly, the splitting value) is comparable to or less than the laser linewidth of 100–150 MHz. Under these conditions, the regime of photoexcitation of atoms turns out to be intermediate between the incoherent and coherent regimes, when oscillations at the Rabi frequency can change phase several times during the laser pulse and regular population oscillations inherent in the coherent regime do not have time to form. In this regime, it is quite correct and justified to use the incoherent approach using effective cross sections to estimate the level population dynamics during photoionisation.

Acknowledgements. The study was supported by a grant from the Russian Science Foundation (Project No. 17-13-01180).

References

1. D'yachkov A.B., Gorkunov A.A., Labozin A.V., Makoveeva K.A., Mironov S.M., Panchenko V.Ya., Firsov V.A., Tsvetkov G.O. *Opt. Spectrosc.*, **128**, 6 (2020) [*Opt. Spektrosk.*, **128**, 10 (2020)]
2. Fedchak J.A., Den Hartog E.A., Lawler J.E., Palmeri P., Quinet P., Biemont E. *Astrophys. J.*, **542**, 1109 (2020).
3. D'yachkov A.B., Gorkunov A.A., Labozin A.V., Mironov S.M., Panchenko V.Ya., Firsov V.A., Tsvetkov G.O. *Quantum Electron.*, **48**, 1043 (2018) [*Kvantovaya Elektron.*, **48**, 1043 (2018)].
4. Autler S.H., Townes C.H. *Phys. Rev.*, **100**, 703 (1955).
5. Shore B. *Acta Phys. Slovaca*, **58**, 243 (2008).
6. Ackerhalt J.R., Eberly J.H., Shore B.W. *Phys. Rev. A*, **19**, 248 (1979).
7. D'yachkov A.B., Gorkunov A.A., Labozin A.V., Mironov S.M., Panchenko V.Ya., Firsov V.A., Tsvetkov G.O. *Quantum Electron.*, **48**, 75 (2018) [*Kvantovaya Elektron.*, **48**, 75 (2018)].
8. D'yachkov A.B., Gorkunov A.A., Labozin A.V., Mironov S.M., Panchenko V.Ya., Firsov V.A., Tsvetkov G.O. *Instrum. Exp. Tech.*, **61**, 548 (2018) [*Prib. Tekh. Eksp.*, (4), 81 (2018)].
9. Białynicka-Birula Z., Białynicki-Birula I., Eberly J.H., Shore B.W. *Phys. Rev. A,* **16**, 2048 (1977).
10. Sobel'man I.I. *Introduction to the Theory of Atomic Spectra* (New York: Pergamon, 1972; Moscow: Fizmatgiz, 1963).
11. Axner O., Gustafsson J.O., Omenetto N., Winefordner J.D. *Spectrochim. Acta. Part B: Atomic Spectrosc.*, **59**, 1 (2004).
12. Berestetskii V.B., Lifshitz E.M., Pitaevskii V.B. *Relativistic Quantum Theory* (Oxford: Pergamon Press, 1974; Moscow: Nauka, 1968) Vol. 4.
13. https://lweb.cfa.harvard.edu/amp/ampdata/kurucz23/sekur.html.
14. Kwiatkowski M., Teppner U., Zimmermann P. *Z. Naturforsch. Sect. A: J. Phys. Sci.*, **35**, 370 (1980).